



1 Quantifying the emission changes and associated air quality impacts during
2 the COVID-19 pandemic in North China Plain: a response modeling study

3 Jia Xing^{1,2}, Siwei Li^{3,4,*}, Yueqi Jiang^{1,2}, Shuxiao Wang^{1,2,*}, Dian Ding^{1,2}, Zhaoxin Dong^{1,2}, Yun Zhu⁵, Jiming Hao^{1,2}

4 ¹ State Key Joint Laboratory of Environmental Simulation and Pollution Control, School of Environment,
5 Tsinghua University, Beijing 100084, China

6 ² State Environmental Protection Key Laboratory of Sources and Control of Air Pollution Complex, Beijing
7 100084, China

8 ³ School of Remote Sensing and Information Engineering, Wuhan University, Wuhan 430079, China

9 ⁴ State Key Laboratory of Information Engineering in Surveying, Mapping and Remote Sensing, Wuhan
10 University, Wuhan 430079, China

11 ⁵ College of Environment and Energy, South China University of Technology, Guangzhou Higher Education
12 Mega Center, Guangzhou 510006, China

13 *Corresponding Authors: Shuxiao Wang (email: shxwang@tsinghua.edu.cn; phone: +86-10-62771466; fax: +86-
14 10-62773650); Siwei Li (email: siwei.li@whu.edu.cn)

15

16 **Abstract**

17 Quantification of emission changes is a prerequisite for the assessment of control effectiveness in
18 improving air quality. However, the traditional bottom-up method for characterizing emissions requires
19 detailed investigation of emissions data (e.g., activity and other emission parameters) that usually takes
20 months to perform and limits timely assessments. Here we propose a novel method to address this issue
21 by using a response model that provides real-time estimation of emission changes based on air quality
22 observations in combination with emission-concentration response functions derived from chemical
23 transport modeling. We applied the new method to quantify the emission changes in the North China Plain
24 (NCP) due to the COVID-19 pandemic shutdown, which overlapped the Spring Festival holiday. Results
25 suggest that the anthropogenic emissions of NO₂, SO₂, VOC, and primary PM_{2.5} in NCP were reduced by
26 51%, 28%, 67% and 63%, respectively, due to the COVID-19 shutdown, indicating longer and stronger
27 shutdown effects in 2020 compared to the previous Spring Festival holiday. The reductions of VOC and



28 primary $\text{PM}_{2.5}$ emissions are generally effective in reducing O_3 and $\text{PM}_{2.5}$ concentrations. However, such
29 air quality improvements are largely offset by reductions in NO_x emissions. NO_x emission reductions lead
30 to increases in O_3 and $\text{PM}_{2.5}$ concentrations in NCP due to the strongly VOC-limited conditions in winter.
31 A strong NH_3 -rich condition is also suggested from the air quality response to the substantial NO_x emission
32 reduction. Well-designed control strategies are recommended based on the air quality response associated
33 with the unexpected emission changes during the COVID-19 period. In addition, our results demonstrate
34 that the new response-based inversion model can well capture emission changes based on variations in
35 ambient concentrations, and thereby illustrate the great potential for improving the accuracy and efficiency
36 of bottom-up emission inventory methods.

37

38 **Keywords:** emission changes, response model, ozone, $\text{PM}_{2.5}$, control effectiveness

39



40 **1. Introduction**

41 Accurate estimation of anthropogenic emissions is crucial for atmospheric modeling studies and
42 provides the basis for developing effective air pollution controls (Wang et al., 2010). A comprehensive
43 emission inventory consists of the emission rates of primary particulate matter components and gaseous
44 pollutants and precursors that are allocated over time and space. These inventories are usually developed
45 using bottom-up methods that gather detailed information about source activity and other emission
46 parameters (Wang et al., 2011; Xing et al., 2015; Li et al., 2017). The challenge is that such investigation
47 is costly and time consuming, and therefore the latest emission inventories usually lag current conditions
48 by a year or more. Many studies also apply a top-down methods to constrain emission estimates using
49 satellite retrievals and modeling methods (Tang et al., 2013, 2019; Lu et al., 2015; Miyazaki et al, 2017;
50 Cao et al., 2018; Zhang et al., 2018). The top-down inversion method can well reflect the change in
51 emissions in a timely manner, and thus efficiently estimate emissions at high spatial and temporal
52 resolution to complement bottom-up inventories. Previous inversion studies have focused on individual
53 pollutants that can be measured directly; however, studies are lacking that use top-down methods to
54 estimate emissions of multiple pollutants, including those that cannot be directly measured, such as
55 primary fine particulate matter (p-PM_{2.5}).

56 The ongoing Coronavirus disease 2019 (COVID-19) pandemic has led to 4,600 deaths in mainland
57 China (by May 24, 2020, <https://news.google.com/covid19/>), and has resulted in a dramatic curtailment
58 of routine economic and social activities. The shutdown of human activities during the COVID-19
59 pandemic has led to reduced pollutant emissions and possibly improved air quality (Shi et al., 2020; Wang
60 et al., 2020a). Yet according to ambient concentration measurements, heavy PM_{2.5} pollution still occurred
61 during the COVID-19 period, and formation of secondary pollutants was actually enhanced in China (Li
62 et al., 2020; Huang et al., 2020). Some studies attributed pollution enhancements to atypical weather
63 conditions that are favorable for air pollution formation (Wang et al., 2020b). Meanwhile, the unexpected



64 reduction of anthropogenic emissions due to the COVID-19 shutdown might vary significantly for
65 different sectors and species. For example, emissions from domestic sources might have increased due to
66 a greater demand for home heating and other essential consumptions during periods with stay-at-home
67 orders in effect. Moreover, the coincidence of the COVID-19 shutdown and the Spring Festival in China
68 resulted in large numbers of people confined to their rural or small-city hometowns, where consumption
69 patterns differ greatly from their primary residence in megacities. Relative to previous years, both
70 emissions and meteorological conditions varied simultaneously during the 2020 COVID-19 shutdown,
71 and an accurate estimation of the changes in anthropogenic emissions accounting for meteorological
72 variations is needed to characterize the impacts of COVID-19 on air quality.

73 Here we propose a novel inversion technique based on a multi-pollutant nonlinear response model
74 to estimate the emission changes in NCP during the COVID-19 shutdown. Emission changes for the
75 COVID-19 period are calculated as the difference between emission estimates for actual conditions and
76 hypothetical conditions assuming the shutdown did not occur. The hypothetical emissions are determined
77 by combining top-down emission estimates from before and after the shutdown with estimates of the
78 temporal variation in emissions from a bottom-up emission inventory. Additionally, we estimate the
79 change in emissions associated with the Spring Festival holiday in 2019 to contrast with results for the
80 combined Spring Festival holiday and COVID-19 shutdown in 2020. Finally, we evaluate the impacts on
81 $PM_{2.5}$ and O_3 concentrations of the combined emission changes and for each emitted species to provide
82 insights for the design of effective control strategies in the future.

83 **2. Methods**

84 **2.1 Response model to estimate the actual emissions from observed surface concentrations**

85 The principle of the new response-based inversion model (hereafter “the response model”) is to
86 adjust the assumed prior emissions such that concentration predictions match observations. The core
87 element of the inversion method is a nonlinear response surface model (RSM) that represents the emission-



88 concentration response functions. The framework of the response model is illustrated in Figure 1. We
89 conduct chemical transport model simulations using prior emissions to get the original simulated
90 concentrations of six pollutants (i.e., NO₂; O₃; SO₂; PM_{2.5}; sulfate, SO₄²⁻; and nitrate, NO₃⁻), as well as the
91 response functions derived from the RSM (Xing et al., 2011; Wang et al., 2011; Xing et al., 2017; 2018).
92 We then adjust the emission ratio of five pollutants (i.e., NO₂, VOC, SO₂, NH₃ and primary PM_{2.5}) to
93 estimate the updated simulated concentrations to match with the observations.

94 Based on our previous knowledge of emission-concentration response relationships, we first adjust
95 NO_x emissions such that RSM predictions match NO₂ observations (see E1), since NO₂ concentrations
96 have a strong linear relationship with NO_x emissions (Xing et al., 2017).

$$97 \quad E'_{NO_x} = r_{NO_x} \times E^*_{NO_x} = E^*_{NO_x} \times \frac{C^o_{NO_2}}{C^s_{NO_2}} \quad (E1)$$

98 where E'_{NO_x} is the adjusted NO_x emissions; $E^*_{NO_x}$ is the prior NO_x emissions; r_{NO_x} is the adjustment ratio
99 for NO_x emissions; $C^o_{NO_2}$ is the observed NO₂ concentrations; and $C^s_{NO_2}$ is the simulated NO₂
100 concentrations.

101 Next, we adjust VOC emissions such that RSM predictions match observed O₃ concentrations, since
102 O₃ concentrations are solely determined by VOC emissions after NO_x emissions are determined in the
103 previous step. The adjusted VOC emission ratio (i.e., $r_{VOC} = E'_{VOC}/E^*_{VOC}$) is determined by solving the
104 following equation E2:

$$105 \quad \Delta O_3 = (C^o_{O_3} - C^s_{O_3}) = RSM_{O_3}(r_{NO_x}, r_{VOC}) \quad (E2)$$

106 where E'_{VOC} is the adjusted VOC emissions; E^*_{VOC} is the prior VOC emissions; ΔO_3 is the difference
107 between observed O₃ concentrations ($C^o_{O_3}$) and simulated O₃ concentrations ($C^s_{O_3}$); and RSM_{O_3} is the
108 response function of O₃ concentrations to NO_x and VOC emissions.

109 Although SO₂ concentrations are linearly related to SO₂ emissions, the chemical transport model
110 overestimates SO₂ concentrations and underestimates SO₄²⁻ concentrations due to large uncertainties in
111 simulating the rapid conversion of SO₂ to SO₄²⁻ during haze episodes (Zhang et al., 2019). To address this



112 deficiency, we adjusted the SO₂ emissions using the observed SO₄²⁻/SO₂ ratio such that the RSM
113 predictions matched both the observed SO₂ and SO₄²⁻ concentrations. Since SO₄²⁻ concentrations are quite
114 linearly related to SO₂ emissions when NH₃ emissions are at moderate levels (Wang et al., 2011), we
115 assume that the unaccounted for SO₂-to-SO₄²⁻ conversion pathway contributes to differences in the
116 observed and simulated SO₄²⁻/SO₂ ratios. Under this assumption, simulated SO₂ concentrations are
117 overestimated by the same ratio (α) that secondary SO₄²⁻ (C_{s-SO4}^s) concentrations are underestimated (see
118 E3 and E4). The primary SO₄²⁻ concentration (C_{p-SO4}^s) was removed from the total SO₄²⁻ concentration in
119 these calculations, because primary SO₄²⁻ is directly emitted and not related to the conversion of SO₂ to
120 SO₄²⁻ (see E4).

$$121 \quad C_{SO_2}^o = \frac{1}{\alpha} \times r_{SO_2} \times C_{SO_2}^s \quad (E3)$$

$$122 \quad C_{SO_4}^o = \alpha \times r_{SO_2} \times C_{s-SO_4}^s + C_{p-SO_4}^s \quad (E4)$$

$$123 \quad \alpha = \left(\frac{C_{SO_2}^o}{C_{SO_4}^o - C_{p-SO_4}^s} / \frac{C_{SO_2}^s}{C_{SO_4}^s} \right)^{1/2} \quad (E5)$$

124 The adjusted SO₂ emission ratio (r_{SO2}) is estimated by taking the ratio of observed SO₂ (C_{SO2}^o) to simulated
125 SO₂ (C_{SO2}^s) multiplied by α, which accounts for the model deficiency in simulating the rapid conversion
126 of SO₂ to SO₄²⁻. For simplification, here we estimate the α value at a domain and temporal averaged level
127 (i.e., identical across the space and time), though such ratio might vary with time and space. The α is
128 smaller than 1 because the observed SO₄²⁻/SO₂ is usually greater than the simulation. The inclusion of the
129 α may help the response model avoid the underestimation of SO₂ emissions.

130 Using the adjusted NO_x, VOC, and SO₂ emissions from previous steps, we next adjusted NH₃
131 emissions such that RSM predictions of NO₃⁻ concentrations matched observations:

$$132 \quad \Delta NO_3^- = (C_{NO_3}^o - C_{NO_3}^s) = RSM_{NO_3}(r_{NO_x}, r_{VOC}, r_{SO_2}, r_{NH_3}) \quad (E6)$$

133 where r_{NH3} = E'_{NH3}/E*_{NH3}, E'_{NH3} is the adjusted NH₃ emissions, and E*_{NH3} is the prior NH₃ emissions.

134 After updating the emissions of the four gaseous precursors, the secondary portion of PM_{2.5} was



135 correspondingly determined, including the secondary organic aerosol contributed by the VOC emissions.
136 Finally, the primary PM_{2.5} emissions were adjusted to provide agreement between simulated and observed
137 total PM_{2.5} concentrations:

$$138 \quad \Delta PM_{2.5} = (C_{PM_{2.5}}^o - C_{PM_{2.5}}^s) = RSM_{PM_{2.5}}(r_{NOx}, r_{VOC}, r_{SO_2}, r_{NH_3}, r_{p-PM_{2.5}}) \quad (E7)$$

139 where $r_{p-PM_{2.5}} = E'_{p-PM_{2.5}}/E_{p-PM_{2.5}}^*$, $E'_{p-PM_{2.5}}$ is the adjusted primary PM_{2.5} emissions, and $E_{p-PM_{2.5}}^*$
140 is the prior primary PM_{2.5} emissions.

141 The prior emissions used here were based on a bottom-up inventory developed for 2017. Since our
142 study focuses on periods in 2019 and 2020, we first use the response model to adjust the 2017 emission
143 inventory to match the two study periods. The first study period was defined as 1 January – 31 March
144 2019 to capture changes in activity due the Spring Festival. The second study period was defined as the
145 same three months in 2020 to capture the COVID-19 shutdown in NCP, which overlapped the 2020 Spring
146 Festival holiday. We defined three sub-periods within the three months in each year as pre-shutdown
147 (Period 1), shutdown (Period 2), and post-shutdown (Period 3). The days selected for sub-periods differed
148 in 2019 and 2020 due to differences in the dates and lengths of the shutdowns. For 2019, we defined
149 Period 1: 1–29 Jan. (29 days); Period 2: 30 Jan. – 18 Feb. (20 days), which is a week before and after the
150 2019 Lunar New Year holidays; and Period 3: 19 Feb. – 31 Mar. (41 days). For 2020, we defined Period
151 1: 1–22 Jan. (22 days); Period 2: 23 Jan. – 5 Mar. (33 days), which is from the date that Chinese authorities
152 began targeted transportation shutdowns until all human activities began recovering in early March
153 (<http://www.gov.cn/index.htm>); and Period 3: 6–31 Mar. (26 days).

154 The RSM was developed using ambient concentrations from simulations with the Community
155 Multiscale Air Quality (CMAQ, version 5.2.1) model, which incorporated meteorological fields from the
156 Weather Research and Forecasting (WRF, version 3.8) model. The WRF-CMAQ system was configured
157 as in our previous studies, and model performance for meteorological variables and pollutant
158 concentrations was evaluated (Ding et al., 2019). The RSM was developed following the same design as



159 our previous study (Xing et al., 2017), in which the polynomial response functions for O₃, PM_{2.5} and PM_{2.5}
160 components were fitted by 40 brute-force CMAQ simulations. Specifically, deep-learning technology was
161 used to fit response surfaces for the three months in 2019 and 2020 using CMAQ simulations for baseline
162 and zero-out emissions conditions (Xing et al., under review) (see Figure 2). The response surfaces were
163 developed using year-specific meteorology based on WRF simulations to account for differences in
164 meteorological conditions between 2019 and 2020.

165 Measurements of ambient concentrations of NO₂, SO₂, O₃ and PM_{2.5} were obtained from the China
166 National Environmental Monitoring Centre (<http://106.37.208.233:20035/>). Measurements of PM_{2.5}
167 chemical components, including NO₃⁻ and SO₄²⁻, were provided by the urban PM data analysis platform
168 in the 2+26 cities of Beijing-Tianjin-Hebei and surrounding regions (<http://106.37.181.120:9011/bfs>). All
169 monitoring data were given as hourly-averaged concentrations at the monitoring sites shown in Figure 2.
170 As in our previous RSM studies, daily daytime O₃ concentrations were analyzed based on afternoon
171 averages (12:00pm-6:00pm local time), and PM_{2.5} concentrations were based on daily 24-hour averages
172 (Xing et al., 2018). Since the monitors sample pollutants at discrete locations and measurements are not
173 available for all days at all sites, provincial average concentrations were used to facilitate adjustments
174 domain-wide for all days in each study period. The provincial average concentrations were calculated
175 using spatially and temporally matched simulated and observed values.

176 **2.2 Hypothetical emissions without shutdown effects**

177 The actual emissions can be derived using observed concentrations and the response model.
178 However, hypothetical emissions under the assumption of no shutdown effects are also needed to estimate
179 the changes in emissions due to the 2019 and 2020 shutdowns. We estimate the hypothetical emissions
180 using the temporal profiles of sectoral emissions from the bottom-up inventory in combination with the
181 derived (actual) emissions for the pre- and post-shutdown periods. We assume that the Spring Festival
182 shutdowns in 2019 have negligible influence on emissions during the periods before and after the



183 shutdown (i.e., Period 1 and Period 3, respectively), while the COVID-19 pandemic in 2020 might have
184 had lag effects after the shutdown due to reduced economic activity or relaxed pollutant controls. However,
185 we concentrate our analysis of COVID-19 impacts on emissions and air quality in the official shutdown
186 period only (Period 2). The hypothetical no-shutdown emissions for Period 2 (noted as Period 2H) are
187 estimated using ratios of emissions for Period 2 and Period 1 and 3 based on the temporal profile of the
188 bottom-up inventory which only reflects the natural evolution of emissions across a year for each sector.
189 This approach develops hypothetical emissions following the typical variation in emissions without
190 shutdown effects. Note that we use the temporal profile to determine the change in Period 2 emissions
191 relative to Period 1 and 3, and so emissions from both Period 1 and 3 are needed to estimate Period 2H
192 emissions.

193 The emission changes due to the COVID-19 shutdown can be estimated by taking the difference of
194 emissions in Period 2, derived from the response model, and emissions in Period 2H, estimated from
195 emissions in Period 1 and 3 using the temporal profile of bottom-up sectoral emissions. The impacts of
196 emission changes during the COVID-19 shutdown on $PM_{2.5}$ and O_3 concentrations are then estimated with
197 the RSM. In addition to the combined impacts of emission changes from multiple species, we estimate the
198 impacts of individual pollutant emissions on $PM_{2.5}$ and O_3 . Due to the nonlinearity of emission-
199 concentration response functions, the impacts of individual pollutant emissions can vary significantly
200 when other pollutant emissions are change simultaneously (Xing et al., 2018). To simplify the evaluation,
201 we define an incremental method for analyzing the individual pollutant impacts in this study by adding
202 incremental changes in pollutant emissions to the previous simulation in the following order: NO_x , VOC,
203 NH_3 , SO_2 and primary $PM_{2.5}$, as described in Table 1. The impacts of individual pollutant emissions on
204 O_3 and $PM_{2.5}$ concentrations are then estimated from the difference between the incrementally adjusted
205 simulation and the previous one. Note that this approach is an approximation, and the impacts of individual
206 pollutants could change if a different order is used.



207 **3. Results**

208 **3.1 Emission changes due to the shutdown**

209 Using the response model, the daily emissions of NO_x, VOC, NH₃, SO₂ and primary PM_{2.5} in NCP
210 are estimated for three periods in 2019 and 2020, as summarized in Figure 3 and detailed in Table 2 by
211 provinces.

212 For Period 1 before the activity disruptions, the emissions of NO_x, SO₂, and VOC in NCP decreased
213 by 11%, 25%, and 8% between 2019 and 2020, respectively. These reductions reflect the progress of air
214 pollution controls between 2019 and 2020, and demonstrate the ability of the model to capture emission
215 changes from routine air pollution control actions. The p-PM_{2.5} emissions also significantly decreased in
216 Beijing-Tianjin-Hebei provinces but increased in Shandong and Henan. The NH₃ emissions did not change
217 during this two-year period, since NH₃ is not considered in current policies.

218 Activity reductions occurred in Period 2 in both 2019 and 2020, although the shutdown due the
219 Spring Festival in 2019 is much shorter than the COVID-19 shutdown in 2020. The emissions of NO_x,
220 SO₂ and p-PM_{2.5} in Period 2 in 2020 are substantially lower than in 2019 (29%, 22% and 73%,
221 respectively). The decreases of NO_x and p-PM_{2.5} for Period 2 between 2019 and 2020 are larger than the
222 decreases for Period 1, which did not experience shutdowns. Such results suggest that the COVID-19
223 shutdown in 2020 had longer and stronger impacts on emissions than the Spring Festival shutdown in
224 2019. Interestingly, emissions of NH₃ and VOC increased significantly (by 5% and 14%) from 2019 to
225 2020 in Period 2. These changes are likely due to the temporal variations of emissions of both species,
226 which are enhanced in warmer months due to stronger evaporation. Period 2 in 2020 extended farther into
227 the Spring (until early March) than Period 2 in 2019, and thus led to increased evaporative emissions of
228 NH₃ and VOC. These results also demonstrate the importance of developing emissions with high temporal
229 resolution.

230 For Period 3 after the shutdown, the decreases of NO_x emissions (14%) are similar to those in Period



231 1 (11%), indicating the recovery of the activity. However, the emissions of VOC and p-PM_{2.5} are much
232 lower in Period 3 in 2020 compared to that in 2019, suggesting the lag effects after the COVID-19
233 shutdown in 2020. In contrast, the small increases of SO₂ emissions in 2020 (2%) might be associated
234 with the extended central heating activity through the end of March in 2020, compared with mid-March
235 in 2019. Higher NH₃ emissions in Period 3 in 2020 than 2019 are also due to the larger coverage of warm
236 days in Period 3 of 2020. NH₃ emissions show the strongest monthly variations among all pollutants
237 (Figure 3). Similarly, increases in VOC emissions are also driven by the change of meteorological
238 conditions (i.e., the higher air temperature in March leads to a larger evaporative emissions), though the
239 growth of VOC emissions from Period 1 to Period 3 is reduced by the COVID-19 shutdown in 2020. Such
240 results also demonstrate that the response model can capture the temporal variations of emissions even in
241 cases where emissions are strongly coupled with meteorological conditions.

242 The influence of the shutdown is estimated as the difference in emissions between Period 2H
243 (hypothetical emissions without shutdown effects) and Period 2 (actual emissions), as shown in Figure 3
244 (grey and red bars respectively) and detailed in Table 3 by NCP province. Due to the COVID-19 shutdown
245 in 2020, emissions of NO_x, VOC and PM_{2.5} decreased substantially by 51%, 67% and 63%, respectively.
246 SO₂ emissions also decreased by 28%, while NH₃ emissions experienced very small increases (+2%)
247 which might be associated with increased activities in rural areas (e.g., potential NH₃ emission sources
248 like stool burning) as many people relocated from megacities to small towns or the countryside. Compared
249 to the effects of the Spring Festival in 2019, the COVID-19 shutdown led to greater reductions in NO_x,
250 SO₂ and PM_{2.5} emissions. The smaller VOC reduction in 2020 compared to 2019 might be due to the
251 difference in temporal coverage of Period 2 in the two years (i.e., there were more warm days in Period 2
252 in 2020). Note that the hypothetical emissions in Period 2H are estimated based on the assumption of no
253 shutdown effects in both Period 1 and Period 3. Therefore the reduction of those pollutant emissions in
254 2020 might be even larger considering the lag effects of COVID-19.



255 3.2 The shutdown effects on ambient concentrations

256 Using the RSM, we predicted concentrations based on the updated emissions from the response-
257 based inversion model. In general, the simulated concentrations based on the adjusted emissions matched
258 well with the observed concentrations, as shown in Figure 4 for NCP averages and detailed by province
259 in Figure S1-12. More important, during the shutdown period in both years, the simulations using adjusted
260 emissions without considering shutdown influences significantly overestimate the NO_2 concentrations in
261 2019 and 2020 by 61% and 81%, respectively. The high-biases in 2019 and 2020 are reduced to within 1%
262 in the simulation with consideration of shutdown effects (Figure 4a).

263 The results for O_3 are quite interesting, as simulated O_3 concentrations are close to observations in
264 both simulations with and without consideration of shutdown influences (Figure 4b). The apparent
265 insensitivity of O_3 concentrations to emission changes during the shutdown can be explained by the
266 nonlinear response of O_3 to its two precursors, NO_x and VOC. In Figure 5a, we compare the response of
267 O_3 concentrations for two NO_x and VOC emission change pathways starting from the hypothetical
268 emissions for no-shutdown conditions (black symbol in Figure 5a). Since NO_x emissions clearly decreased
269 due to the shutdown, the O_3 concentrations would increase if VOC emissions remained constant
270 (following the green line to the green symbol in Figure 5a). Yet the simulation without consideration of
271 VOC emission changes would result in a high bias of simulated O_3 concentrations compared to the
272 observations by 49% in 2019 and 29% in 2020. The low observed O_3 concentrations during Period 2 in
273 both years indicates that VOC emission reductions must have occurred to maintain the suppressed O_3 level
274 (following the red line to the red symbol in Figure 5a). Consistent with this interpretation, the simulated
275 O_3 concentrations agree well with observations (e.g., normalized mean bias, $\text{NMB} < 3\%$) when both NO_x
276 and VOC emission reductions are represented.

277 The substantial reduction of NO_x emissions also resulted in noticeable decreases in NO_3^-
278 concentrations (black and green lines in Figure 4c). However, the low bias in NO_3^- predictions cannot be



279 readily mitigated by adjusting the NH_3 emissions, because the substantial decreases in NO_x emissions
280 associated with the shutdown result in a strong NH_3 -rich conditions, where NO_3^- concentrations are less
281 sensitive to NH_3 emissions increases. The response of NO_3^- concentrations to pathways of NO_x and NH_3
282 emission changes is depicted in Figure 5b (SO_2 and VOC emissions are also changing simultaneously with
283 NO_x). A larger decrease in simulated than observed NO_3^- concentrations is associated with the NO_x
284 emission reductions, but the change of NH_3 emissions can hardly increase the NO_3^- concentrations under
285 such strong NH_3 -rich conditions. Therefore, the model predicted no NH_3 changes in 2019, but very small
286 increases of NH_3 emissions (+2%) in 2020 due to the increased activities in rural areas which slightly
287 reduced the NO_3^- low biases (NMB from -12% to -11%).

288 The large reduction in SO_2 emissions estimated with the response model during the 2020 shutdown
289 considerably reduced the high biases in simulated SO_2 and SO_4^{2-} concentrations (Figure 4d-f). However,
290 the SO_4^{2-} biases are still considerable after the emission adjustment because a large fraction of SO_4^{2-} might
291 come from primary sources, which need further investigation especially for its contribution to p- $\text{PM}_{2.5}$.

292 Agreement between the simulated and observed $\text{PM}_{2.5}$ concentrations also improves when
293 accounting for the reductions in primary $\text{PM}_{2.5}$ emissions estimated with the response model in both years
294 (Figure 4g). Another interesting finding is that the simulated $\text{PM}_{2.5}$ concentrations with consideration of
295 all emission changes due to the shutdown (red line in Figure 4g) are quite similar to $\text{PM}_{2.5}$ predictions
296 without consideration of the shutdown impacts (black line in Figure 4g). The same behavior is evident for
297 O_3 concentrations (red and black lines in Figure 4b). As discussed above, the reductions in emissions of
298 multiple species during the shutdown had compensating influences on air quality, and the overall effects
299 of the emission changes on O_3 and $\text{PM}_{2.5}$ concentrations were neutralized to a relatively small level.

300 **3.3 Impacts of individual emission changes from the shutdown on O_3 and $\text{PM}_{2.5}$ concentrations**

301 To further investigate the individual impacts of emission changes of each pollutant on O_3 and $\text{PM}_{2.5}$
302 concentrations, we conducted sensitivity analysis by sequentially adding each incremental emission



303 change into the model system and then calculating the associated changes in O_3 and $PM_{2.5}$ concentrations.
304 By incrementally adding the impacts of emission changes of five pollutants (ΔNO_x , ΔVOC , ΔNH_3 , ΔSO_2 ,
305 and $\Delta p-PM_{2.5}$), the concentrations change from the original simulation, without consideration of shutdown
306 impacts (noted as oSIM, shown as grey bar in Figure 6), and ultimately reaching the observed levels (noted
307 as OBS, shown as narrow blue bars in Figure 6).

308 For O_3 , the reduction of NO_x emissions lead to a significant enhancement of O_3 (see ΔNO_x) due to
309 the VOC-limited regime in winter (Xing et al., 2019), while such O_3 enhancement has been largely or
310 completely mitigated thanks to the simultaneous reduction of VOC emissions (see ΔVOC) in both 2019
311 and 2020. This behavior is particularly evident in Henan and Shandong provinces which experienced
312 substantial VOC reductions during the shutdown (Table 3). Such benefits from simultaneous VOC
313 controls also occurred for $PM_{2.5}$ concentrations. Compared with O_3 , the changes in $PM_{2.5}$ concentrations
314 are more complex to interpret due to the influence of emission changes for SO_2 (ΔSO_2), NH_3 (ΔNH_3) and
315 $p-PM_{2.5}$ ($\Delta p-PM_{2.5}$) in addition to NO_x and VOC. Results suggest that the reductions of $p-PM_{2.5}$ emissions
316 tended to favor $PM_{2.5}$ decreases while the ΔSO_2 and ΔNH_3 emission changes have negligible influence.
317 Overall, reductions in $p-PM_{2.5}$ and VOC emissions helped mitigate potential $PM_{2.5}$ concentration
318 enhancements in most NCP provinces. Similar findings are suggested in Hang et al. (2020), which
319 observed enhanced secondary pollution during the COVID-19 period. The air quality impacts from the
320 unexpected controls during the COVID-19 shutdown suggest that strengthened controls on $p-PM_{2.5}$
321 emissions and well-balanced reductions in NO_x and VOC emissions would be an effective strategy for
322 further improving air quality in NCP (Xing et al., 2018).

323 4. Summary and Conclusion

324 In summary, this study developed a response-based inversion modeling framework and applied it to
325 characterize the emission changes and associated air quality impacts during the 2019 Spring Festival and
326 the 2020 COVID-19 pandemic shutdown. Our results indicate that the response model can effectively



327 adjust the assumed prior emissions such that air quality predictions match well with observed
328 concentrations. The model also captures the temporal variations of emissions associated with changes in
329 meteorological conditions. The model may suffer some uncertainties from deficiencies in model chemical
330 mechanisms (e.g., conversion of SO_2 to SO_4^{2-}), as well as the quality of prior emissions and limited
331 coverage of observations. Difficulties are also found in estimating the NH_3 emission changes under strong
332 NH_3 -rich conditions by using the current inversion method based on the concentration of PM chemical
333 components. However, with the continued growth in observational datasets from both surface monitors
334 and satellite retrievals, improvements in knowledge of atmospheric science, and development of advanced
335 assimilation technologies, the new response-based inversion model has great potential to further improve
336 the accuracy and efficiency of emission inventory updates. The importance of reliable bottom-up
337 inventories for defining prior emissions by sector, combined with the ability of the top-down inversion
338 model to rapidly adjust emissions for consistency with observations, demonstrates how bottom-up and
339 top-down emissions modeling methods are complementary.

340 The response model was applied in investigating the emission changes during the COVID-19
341 shutdown. The emission changes were estimated by comparing emissions for actual conditions with
342 emissions for hypothetical conditions assuming that the shutdown did not occur. Emission levels during
343 the COVID-19 shutdown period were estimated by applying the temporal profiles of sectoral emissions
344 from the bottom-up inventory. These estimates may suffer some uncertainties associated with the temporal
345 profiles and the assumption of no shutdown impacts during the post-shutdown period. Our results suggest
346 that the shutdowns in 2019 and 2020 had considerable impacts on air pollutant emissions. Longer and
347 stronger impacts are found in 2020 due to the COVID-19 pandemic compared to the Spring Festival of
348 the previous year. The anthropogenic emissions of NO_2 , SO_2 , VOC, and primary $\text{PM}_{2.5}$ in NCP were
349 reduced by 51%, 28%, 67% and 63%, respectively, due to the COVID-19 shutdown in 2020. The estimated
350 ratio might be slightly underestimated considering the lag effects after the COVID-19 shutdown. We also



351 found that emission changes associated with the shutdown periods had limited impacts on surface O₃ and
352 PM_{2.5} concentrations due to compensating effects of emission changes in different pollutants. Based on
353 our analysis, careful controls on NO_x emission sources in NCP are recommended in combination with
354 simultaneous controls on VOC and NH₃ sources. Such a comprehensive strategy would minimize the
355 potential negative impacts on air quality of NO_x emission reductions during VOC-limited conditions in
356 winter. This study also illustrates that air quality improvements do not necessary follow from precursor
357 emission reductions, and multi-pollutant nonlinear response models are therefore critical tools for
358 representing the nonlinear relationship between emissions and concentrations in designing effective
359 control strategies.

360

361 **Data and code availability**

362 The original data and code used in this study are available upon request from the corresponding
363 authors.

364 **Author contribution**

365 JX & SL designed the methodology, conducted the analysis, and wrote the original draft. YJ
366 conducted the WRF-CMAQ simulation. SW & DD & ZD & JH helped with the bottom-up emission
367 inventory. YZ helped with the RSM model. All authors contribute to writing the paper.

368 **Acknowledgements**

369 This work was supported in part by National Key R & D program of China (2018YFC0213805),
370 and National Natural Science Foundation of China (21625701, 41907190). This work was completed on
371 the “Explorer 100” cluster system of Tsinghua National Laboratory for Information Science and
372 Technology. We thank Drs. Carey Jang, James Kelly, Jian Gao, and Jingnan Hu for contributions to the
373 study. The authors gratefully acknowledge the free availability and use of observation datasets.



374 **Competing interests**

375 The authors declare no competing financial interests.



376 Reference

- 377 Cao, H., Fu, T.-M., Zhang, L., Henze, D. K., Miller, C. C., Lerot, C., Abad, G. G., De Smedt, I., Zhang,
378 Q., van Roozendaal, M., Hendrick, F., Chance, K., Li, J., Zheng, J., and Zhao, Y.: Adjoint inversion of
379 Chinese non-methane volatile organic compound emissions using space-based observations of
380 formaldehyde and glyoxal, *Atmos. Chem. Phys.*, 18, 15017–15046, [https://doi.org/10.5194/acp-18-](https://doi.org/10.5194/acp-18-15017-2018)
381 15017-2018, 2018.
- 382 Ding, D., Xing, J., Wang, S., Liu, K., & Hao, J. (2019). Estimated contributions of emissions controls,
383 meteorological factors, population growth, and changes in baseline mortality to reductions in ambient
384 PM 2.5 and PM 2.5-related mortality in China, 2013–2017. *Environmental health perspectives*, 127(6),
385 067009.
- 386 Huang, X., Ding, A., Gao, J., Zheng, B., Zhou, D., Qi, X., ... & Wang, J. (2020). Enhanced secondary
387 pollution offset reduction of primary emissions during COVID-19 lockdown in China.
- 388 Li, Li, et al. "Air quality changes during the COVID-19 lockdown over the Yangtze River Delta Region:
389 An insight into the impact of human activity pattern changes on air pollution variation." *Science of The*
390 *Total Environment* (2020): 139282.
- 391 Li, M., Zhang, Q., Kurokawa, J. I., Woo, J. H., He, K., Lu, Z., ... & Cheng, Y. (2017). MIX: a mosaic
392 Asian anthropogenic emission inventory under the international collaboration framework of the MICS-
393 Asia and HTAP. *Atmospheric Chemistry and Physics* (Online), 17(2).
- 394 Lu, Z., Streets, D. G., de Foy, B., Lamsal, L. N., Duncan, B. N., and Xing, J.: Emissions of nitrogen
395 oxides from US urban areas: estimation from Ozone Monitoring Instrument retrievals for 2005–2014,
396 *Atmos. Chem. Phys.*, 15, 10367–10383, <https://doi.org/10.5194/acp-15-10367-2015>, 2015.
- 397 Miyazaki, K., Eskes, H., Sudo, K., Boersma, K. F., Bowman, K., and Kanaya, Y.: Decadal changes in
398 global surface NO_x emissions from multi-constituent satellite data assimilation, *Atmos. Chem. Phys.*,
399 17, 807-837, <https://dx.doi.org/doi:10.5194/acp-17-807-2017>, 2017.
- 400 Shi, X., Brasseur, G.P.: The Response in Air Quality to the Reduction of Chinese Economic Activities
401 during the COVID-19 Outbreak, *Geophysical Research Letters*, 2020.
- 402 Tang, W., Arellano, A. F., Gaubert, B., Miyazaki, K., and Worden, H. M.: Satellite data reveal a common
403 combustion emission pathway for major cities in China, *Atmos. Chem. Phys.*, 19, 4269-4288,
404 <https://doi.org/10.5194/acp-19-4269-2019>, 2019.
- 405 Tang, W., Cohan, D. S., Lamsal, L. N., Xiao, X., and Zhou, W.: Inverse modeling of Texas NO_x
406 emissions using space-based and ground-based NO₂ observations, *Atmos. Chem. Phys.*, 13, 11005–
407 11018, <https://doi.org/10.5194/acp-13-11005-2013>, 2013.
- 408 Wang, P., Chen, K., Zhu, S., Wang, P., & Zhang, H. (2020). Severe air pollution events not avoided by
409 reduced anthropogenic activities during COVID-19 outbreak. *Resources, Conservation and Recycling*,
410 158, 104814.



- 411 Wang, S., Xing, J., Chatani, S., Hao, J., Klimont, Z., Cofala, J., & Amann, M. (2011). Verification of
412 anthropogenic emissions of China by satellite and ground observations. *Atmospheric*
413 *Environment*, 45(35), 6347-6358.
- 414 Wang, S., Xing, J., Jang, C., Zhu, Y., Fu, J. S., & Hao, J. (2011). Impact assessment of ammonia
415 emissions on inorganic aerosols in East China using response surface modeling technique.
416 *Environmental science & technology*, 45(21), 9293-9300.
- 417 Wang, S., Zhao, M., Xing, J., Wu, Y., Zhou, Y., Lei, Y., ... & Hao, J. (2010). Quantifying the air
418 pollutants emission reduction during the 2008 Olympic Games in Beijing. *Environmental science &*
419 *technology*, 44(7), 2490-2496.
- 420 Wang, Q., Su, M.: A preliminary assessment of the impact of COVID-19 on environment – A case study
421 of China, *Science of The Total Environment*, 728, 2020
- 422 Xing, J., Wang, S. X., Jang, C., Zhu, Y., & Hao, J. M. (2011). Nonlinear response of ozone to precursor
423 emission changes in China: a modeling study using response surface methodology. *Atmos. Chem. Phys.*,
424 11(10), 5027-5044.
- 425 Xing, J. P. J. M. R., Pleim, J., Mathur, R., Pouliot, G., Hogrefe, C., Gan, C. M., & Wei, C. (2013).
426 Historical gaseous and primary aerosol emissions in the United States from 1990 to 2010. *Atmospheric*
427 *Chemistry & Physics*, 13(15).
- 428 Xing, J., Wang, S., Zhao, B., Wu, W., Ding, D., Jang, C., ... & Hao, J. (2017). Quantifying nonlinear
429 multiregional contributions to ozone and fine particles using an updated response surface modeling
430 technique. *Environmental science & technology*, 51(20), 11788-11798.
- 431 Xing, J., Ding, D., Wang, S., Zhao, B., Jang, C., Wu, W., ... & Hao, J. (2018). Quantification of the
432 enhanced effectiveness of NO_x control from simultaneous reductions of VOC and NH₃ for reducing
433 air pollution in the Beijing–Tianjin–Hebei region, China. *Atmospheric Chemistry and Physics*, 18(11),
434 7799-7814.
- 435 Xing, J., Ding, D., Wang, S., Dong, Z., Kelly, J. T., Jang, C., ... & Hao, J. (2019). Development and
436 application of observable response indicators for design of an effective ozone and fine-particle pollution
437 control strategy in China. *Atmospheric Chemistry and Physics*, 19(21), 13627-13646.
- 438 Xing, et al., Deep learning for prediction of the air quality response to emission changes, under review
- 439 Zhang, L., Chen, Y., Zhao, Y., Henze, D. K., Zhu, L., Song, Y., ... & Huang, B. (2018). Agricultural
440 ammonia emissions in China: reconciling bottom-up and top-down estimates, *Atmos. Chem. Phys.*, 18,
441 339–355, 2018.
- 442 Zhang, S., Xing, J., Sarwar, G., Ge, Y., He, H., Duan, F., ... & Chu, B. (2019). Parameterization of
443 heterogeneous reaction of SO₂ to sulfate on dust with coexistence of NH₃ and NO₂ under different
444 humidity conditions. *Atmospheric environment*, 208, 133-140.
- 445



446 **Table 1** Sensitivity analysis for quantifying the impacts of individual pollutant emission changes on air
447 quality

No.	Emission	Objective	Noted
Sim-1	All pollutants are used as the hypothetical emissions of Period 2H	To estimate the hypothetical concentrations without COVID impacts	Δ oSIM
Sim-2	Same as Sim-1 except NO _x emissions are updated to actual emissions in Period 2	To estimate the impacts of NO _x emission changes on O ₃ and PM _{2.5} based on the difference between Sim-2 and Sim-1	Δ NO _x
Sim-3	Same as Sim-2 except VOC emissions are updated to actual emissions in Period 2	To estimate the impacts of VOC emission changes on O ₃ and PM _{2.5} based on the difference between Sim-3 and Sim-2	Δ VOC
Sim-4	Same as Sim-3 except NH ₃ emissions are updated to actual emissions in Period 2	To estimate the impacts of NH ₃ emission changes on PM _{2.5} based on the difference between Sim-4 and Sim-3	Δ NH ₃
Sim-5	Same as Sim-4 except SO ₂ emissions are updated to actual emissions in Period 2	To estimate the impacts of SO ₂ emission changes on PM _{2.5} based on the difference between Sim-5 and Sim-4	Δ SO ₂
Sim-6	Same as Sim-5 except primary PM _{2.5} emissions are updated to actual emissions in Period 2	To estimate the impacts of primary PM _{2.5} emission changes on PM _{2.5} based on the difference between Sim-6 and Sim-5	Δ p-PM _{2.5}

448

449



450 **Table 2** Daily emissions of five pollutants in NCP provinces based on the response model (unit: kt/day)

2019	Period 1 (29 days, Jan 1 to Jan 29)					Period 2 (20 days, Jan 30 to Feb 18)					Period 3 (41 days, Feb 19 to Mar 31)				
	NO _x	SO ₂	NH ₃	VOC	p-PM _{2.5}	NO _x	SO ₂	NH ₃	VOC	p-PM _{2.5}	NO _x	SO ₂	NH ₃	VOC	p-PM _{2.5}
Beijing	0.49	0.07	0.20	0.69	0.12	0.26	0.05	0.19	0.20	0.01	0.48	0.05	0.23	0.94	0.16
Tianjin	0.65	0.17	0.15	0.92	0.05	0.42	0.17	0.15	0.24	0.04	0.79	0.21	0.25	1.37	0.15
Hebei	5.64	2.01	1.18	3.67	1.97	3.47	1.62	1.27	1.43	1.51	5.95	1.90	2.77	6.26	1.92
Shandong	7.35	3.21	1.34	8.58	0.76	4.45	2.88	1.52	2.41	0.88	6.90	3.45	3.54	9.59	1.19
Henan	5.34	1.49	1.31	4.08	1.54	3.04	1.31	1.74	0.71	1.84	4.46	1.84	4.27	4.46	1.33
NCP	19.47	6.96	4.17	17.94	4.43	11.65	6.03	4.87	5.00	4.28	18.58	7.45	11.07	22.62	4.76

451
 452

2020	Period 1 (22 days, Jan 1 to Jan 22)					Period 2 (33 days, Jan 23 to Mar 5)					Period 3 (26 days, Mar 6 to Mar 31)				
	NO _x	SO ₂	NH ₃	VOC	p-PM _{2.5}	NO _x	SO ₂	NH ₃	VOC	p-PM _{2.5}	NO _x	SO ₂	NH ₃	VOC	p-PM _{2.5}
Beijing	0.38	0.04	0.20	0.65	0.01	0.23	0.03	0.20	0.27	0.01	0.28	0.04	0.24	0.70	0.09
Tianjin	0.64	0.12	0.15	0.87	0.02	0.44	0.12	0.17	0.44	0.03	0.71	0.18	0.30	1.20	0.10
Hebei	5.28	1.34	1.18	3.12	1.73	3.15	1.16	1.54	1.92	0.81	4.97	1.67	3.49	4.72	0.75
Shandong	6.57	2.55	1.34	8.02	0.85	3.28	2.25	1.88	2.44	0.16	5.87	3.57	4.52	8.44	0.14
Henan	4.50	1.15	1.31	3.84	2.26	1.13	1.14	1.31	0.64	0.16	4.09	2.13	5.49	3.13	0.10
NCP	17.37	5.19	4.17	16.51	4.88	8.23	4.69	5.10	5.71	1.17	15.93	7.59	14.03	18.18	1.19
Δ2020-2019	-11%	-25%	0%	-8%	10%	-29%	-22%	5%	14%	-73%	-14%	2%	27%	-20%	-75%

453
 454

(p-PM_{2.5} = primary PM_{2.5})



455 **Table 3** The shutdown-impacts on the emission of five pollutants in NCP provinces

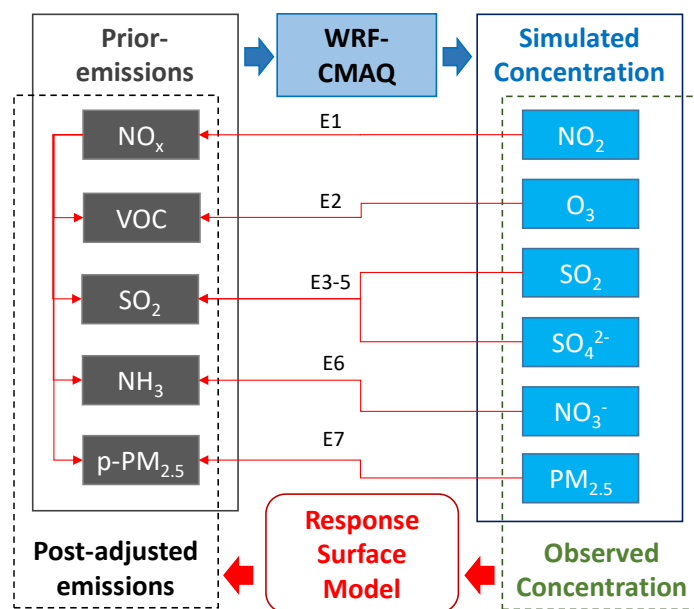
2019	NO _x		SO ₂		NH ₃		VOC		p-PM _{2.5}	
	kt/Day	%	kt/Day	%	kt/Day	%	kt/Day	%	kt/Day	%
Beijing	-0.23	-47%	-0.01	-21%	0.00	0%	-0.56	-73%	-0.15	-93%
Tianjin	-0.30	-41%	-0.02	-10%	0.00	0%	-0.95	-80%	-0.07	-62%
Hebei	-2.33	-40%	-0.34	-17%	0.00	0%	-3.54	-71%	-0.51	-25%
Shandong	-2.67	-37%	-0.46	-14%	0.00	0%	-6.78	-74%	-0.10	-10%
Henan	-1.85	-38%	-0.48	-27%	0.00	0%	-3.39	-83%	0.39	27%
NCP	-7.38	-39%	-1.31	-18%	0.00	0%	-15.23	-75%	-0.43	-9%

456

2020	NO _x		SO ₂		NH ₃		VOC		p-PM _{2.5}	
	kt/Day	%	kt/Day	%	kt/Day	%	kt/Day	%	kt/Day	%
Beijing	-0.10	-30%	-0.01	-18%	0.00	2%	-0.39	-59%	-0.07	-85%
Tianjin	-0.24	-35%	-0.03	-18%	0.00	2%	-0.60	-58%	-0.04	-59%
Hebei	-1.98	-39%	-0.31	-21%	0.03	2%	-1.89	-50%	-0.43	-35%
Shandong	-2.95	-47%	-0.75	-25%	0.04	2%	-5.80	-70%	-0.31	-66%
Henan	-3.16	-74%	-0.76	-40%	0.03	2%	-3.10	-83%	-1.10	-87%
NCP	-8.42	-51%	-1.85	-28%	0.10	2%	-11.77	-67%	-1.95	-63%

457

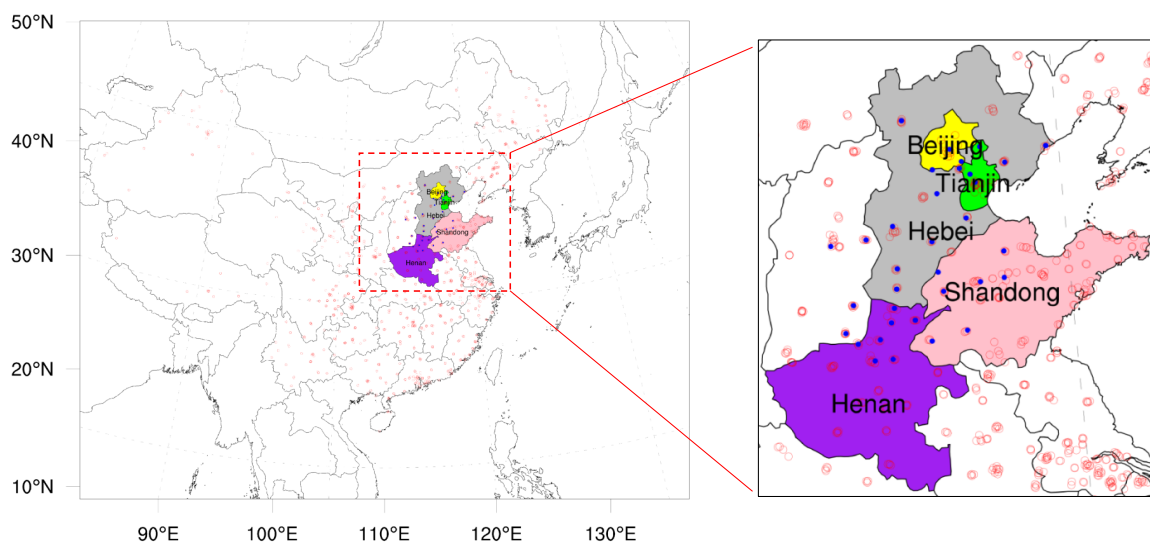
458 (p-PM_{2.5} = primary PM_{2.5})



459

460 **Figure 1** The response modeling framework for adjusting the emissions (the E1-7 are equations used to
461 adjusted emissions, which are detailed in the text)

462



463

464

465

466

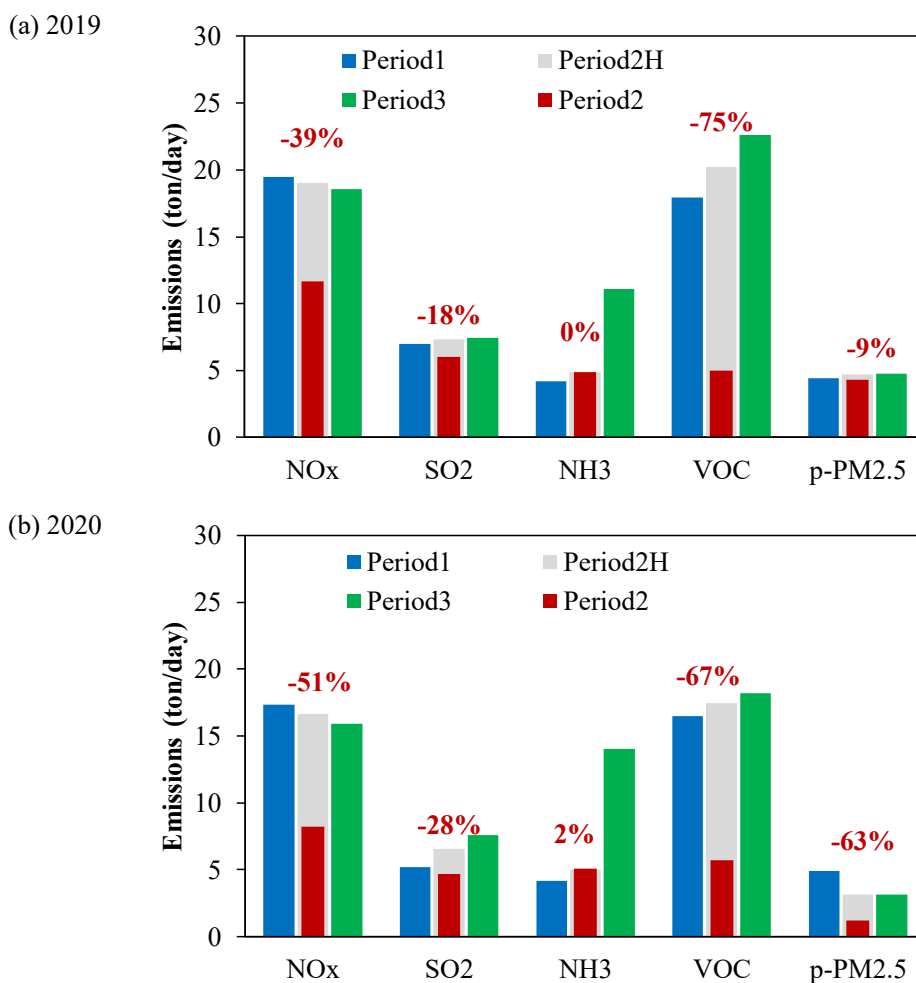
467

Figure 2 Simulation domain and observation sites in five provinces of North China Plain (red dots: surface monitor sites for NO₂, SO₂, O₃ and PM_{2.5}; blue dots: monitor sites for PM_{2.5} chemical components)



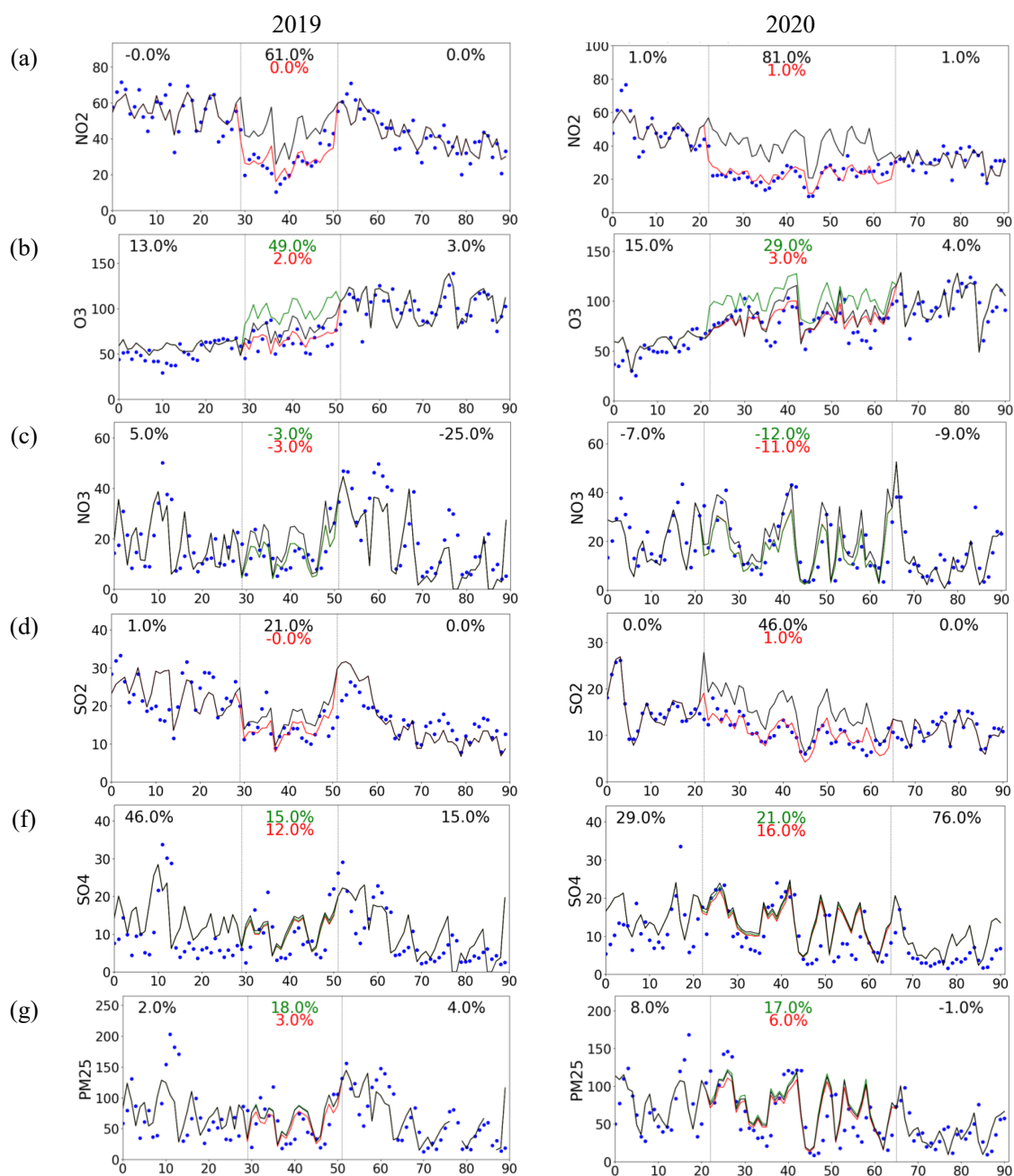
468

469



470 **Figure 3** Daily emissions during pre-shutdown (Period 1, blue), shutdown (Period 2, red), and post-
471 shutdown (Period 3, green) periods in 2019 and 2020. Period 2H (grey) is the hypothetical emissions
472 without reduced activity during the 2019 holiday or 2020 COVID-19 shutdown; the red number
473 indicates the percent change in emissions due to the shutdown in Period 2.

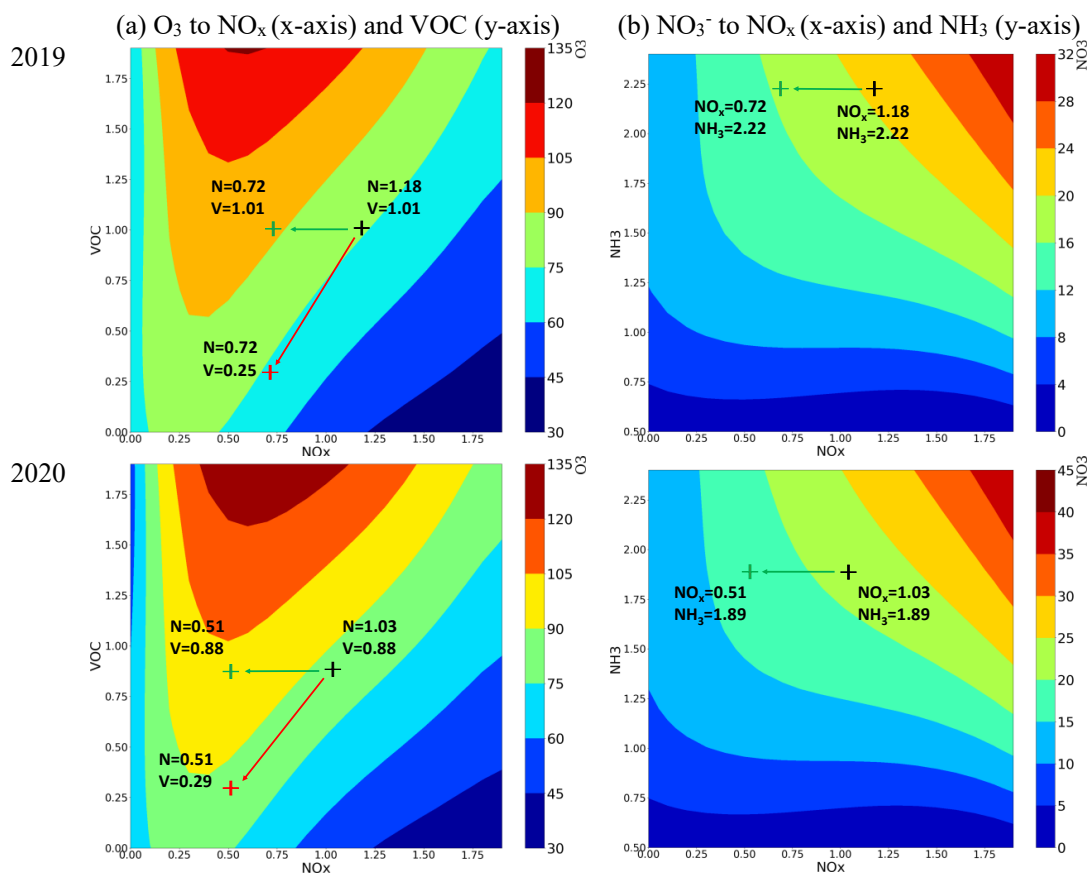
474



475 **Figure 4** Comparison of the simulated and observed average concentrations in NCP (the percentage
 476 numbers indicate the normalized mean biases in hypothesis and actual simulations respectively for
 477 Period 2. Blue dots: observations; Black line: simulations using adjusted emission with no consideration
 478 of shutdown influences; Red line: simulations using adjusted emission with consideration of shutdown
 479 influences; Green line: simulations using adjusted emission with consideration of shut-down
 480 influences without VOC for O₃, NH₃ for NO₃⁻, SO₂ for SO₄²⁻, primary PM_{2.5} for PM_{2.5}; unit: μg m⁻³)



481



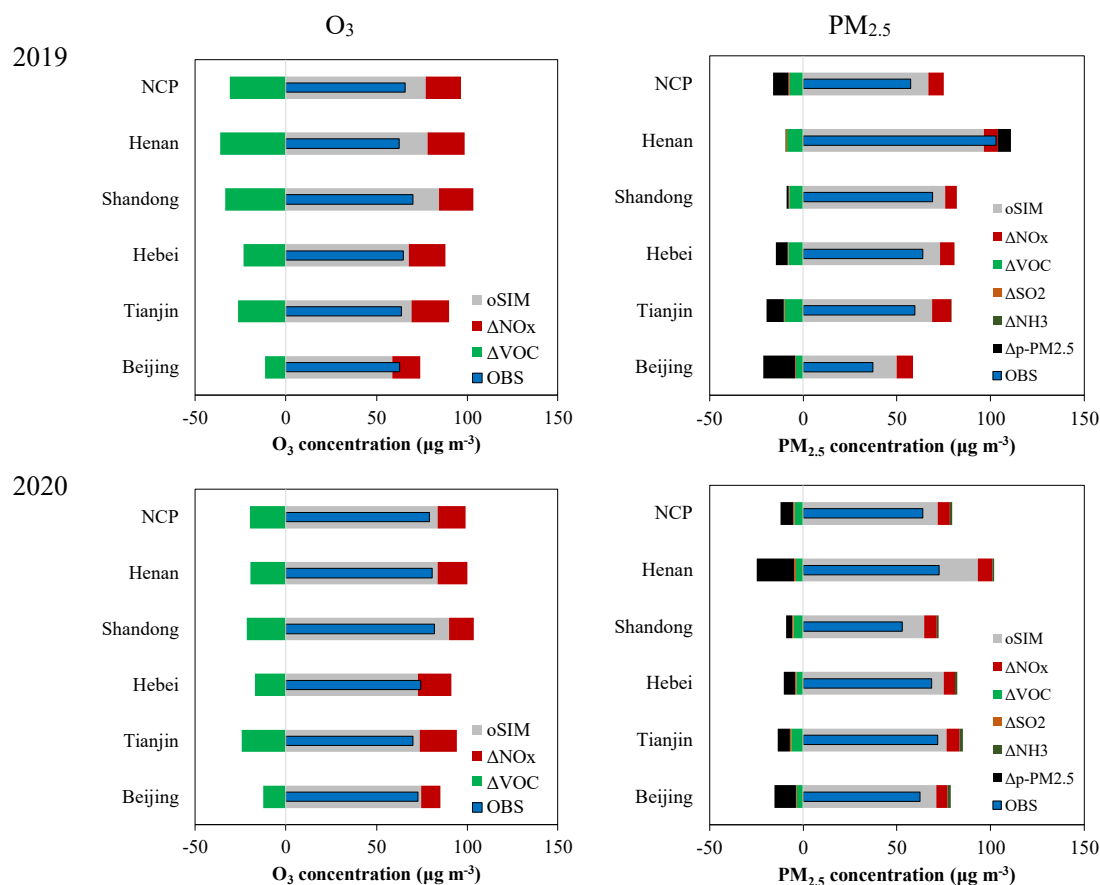
482

483 **Figure 5** Implication of emission changes from the O₃ and NO₃⁻ response isopleths during shutdowns
 484 (the axes indicate emission ratios relative to the prior emissions; black symbol: adjusted emission ratios
 485 with no consideration of shutdown; red symbol: adjusted emission ratios with consideration of
 486 shutdown; green symbol: adjusted emission ratios without considering simultaneous VOC changes for O₃,
 487 and NH₃ changes for NO₃⁻; background color: O₃ and NO₃⁻ concentrations, μg m⁻³)

488



489



490

491 **Figure 6** Contributions to the changes of O₃ and PM_{2.5} concentrations during Period-2 (OBS:
 492 observation; oSIM: no consideration of shutdown; ΔNO_x: impacts due to the change of NO_x emissions;
 493 ΔVOC: impacts due to the change of VOC emissions; ΔNH₃: impacts due to the change of NH₃
 494 emissions; ΔSO₂: impacts due to the change of SO₂ emissions; Δp-PM_{2.5}: impacts due to the change of
 495 primary PM_{2.5} emissions)